GeoHealth

RESEARCH ARTICLE
10.1029/2020GH000292

Special Section:
The COVID-19 Pandemic: Linking Health, Society and Environment

A Warm Summer is Unlikely to Stop Transmission of COVID-19 Naturally

Ming Su[1,2], Shushi Peng[3], Lili Chen[4], Bin Wang[5,6], Ying Wang[7,8], Xiarui Fan[7], and Zhaomin Dong[7,8]

[1]Key Laboratory of Drinking Water Science and Technology, Research Center for Eco-Environmental Sciences, Chinese Academy of Sciences, Beijing, China, [2]College of Resources and Environment, University of Chinese Academy of Science, Beijing, China, [3]Sino-French Institute for Earth System Science, College of Urban and Environmental Sciences, and Laboratory for Earth Surface Processes, Peking University, Beijing, China, [4]Beijing Academy of Edge Computing (BAEC), Beijing, China, [5]Institute of Reproductive and Child Health, Peking University, Beijing, China, [6]Key Laboratory of Reproductive Health, National Health Commission of the People's Republic of China, Beijing, China, [7]School of Space and Environment, Beihang University, Beijing, China, [8]Beijing Advanced Innovation Center for Big Data-Based Precision Medicine, Beihang University, Beijing, China

Abstract The outbreak of coronavirus disease 2019 (COVID-19) showed various transmission rate (R_t) across different regions. The determination of the factors affecting transmission rate is urgent and crucial to combat COVID-19. Here we explored variation of R_t between 277 regions across the globe and the associated potential socioeconomic, demographic, and environmental factors. At global scale, the R_t started to decrease approximately 2 weeks after policy interventions initiated. This lag from the date of policy interventions initiation to the date when R_t started to decrease ranges from 9 to 19 days, largest in Europe and North America. We find that proportion of elderly people or life expectancy can explain ~50% of variation in transmission rate across the 277 regions. The transmission rate at the point of inflection (R_I) increases by 29.4% (25.2–34.0%) for 1% uptick in the proportion of people aged above 65, indicating that elderly people face ~2.5 times higher infection risk than younger people. Air temperature is negatively correlated with transmission rate, which is mainly attributed to collinearities between air temperature and demographic factors. Our model predicted that temperature sensitivity of R_I is only −2.7% (−5.2–0%) per degree Celsius after excluding collinearities between air temperature and demographic factors. This low temperature sensitivity of R_I suggests that a warm summer is unlikely to impede the spread of COVID-19 naturally.

Key Points:
- Timeline of COVID-19 outbreak in 277 regions across the globe was summarized
- Proportion of elderly people or life expectancy can explain 50% of variation in transmission rate of COVID-19 across the 277 regions
- Temperature sensitivity of transmission rate at inflection point is estimated to be −2.7% (−5.2% to 0%) per degree Celsius

Supporting Information:
- Supporting Information S1

Correspondence to:
S. Peng and Z. Dong,
speng@pku.edu.cn;
dongzm@buaa.edu.cn

Citation:
Su, M., Peng, S., Chen, L., Wang, B., Wang, Y., Fan, X., & Dong, Z. (2020). A warm summer is unlikely to stop transmission of COVID-19 naturally. *GeoHealth*, *4*, e2020GH000292. https://doi.org/10.1029/2020GH000292

Received 17 JUN 2020
Accepted 9 OCT 2020

Author Contributions:
Conceptualization: Ming Su, Shushi Peng, Zhaomin Dong
Data curation: Lili Chen, Bin Wang, Ying Wang, Xiarui Fan
Formal analysis: Ming Su, Shushi Peng, Zhaomin Dong
Funding acquisition: Ming Su, Shushi Peng, Ying Wang, Zhaomin Dong
(continued)

1. Introduction

The 2019 coronavirus disease (COVID-19) outbreak caused by severe acute respiratory syndrome coronavirus-2 (SARS-CoV-2) has become an unfolding pandemic, with more than 3.8 million cases being reported up until 8 May 2020 (Dong et al., 2020). Since the outbreak of COVID-19, transmission rate of COVID-19 has evolved with time. The transmission rate at the same stage of outbreak varies by 3–4 orders of magnitude between different regions (https://ourworldindata.org/coronavirus-data; https://coronavirus.jhu.edu/). To eliminate this major public health hazard, it is essential to understand the timeline of evolution in transmission rate for each region. Meanwhile, understanding why the transmission rate varies across different regions can hint clues about how to control the COVID-19 pandemic; thus, investigation on the potential driving factors of COVID-19 transmission across different regions is an urgent and essential mission. This is the main goal of this study.

Previous studies have reported that the policy interventions, meteorological conditions, demography, and healthcare facilities have impacts on the transmission of COVID-19 by experiments, statistics, and mathematical modeling (Chinazzi et al., 2020; Kucharski et al., 2020). Several studies have evaluated the effects of different policy interventions on transmission rate of COVID-19 (Dehning et al., 2020; Kraemer et al., 2020; Tian et al., 2020). In vitro data have confirmed the reduced survival of SARS-CoV-2 with increase in air temperature and relative humidity (Jüni et al., 2020; NAS, 2020; Zhu & Xie, 2020). Meanwhile, elderly people are found sensitive to the COVID-19 by 8,579 case studies in China (Zhang et al., 2020) and susceptible-infected-recovered (SIR) models (Dehning et al., 2020). Logically, better healthcare and richer regions with higher

Investigation: Ming Su, Shushi Peng, Lili Chen, Xiarui Fan
Methodology: Ming Su, Shushi Peng, Zhaomin Dong
Validation: Ming Su, Shushi Peng, Bin Wang
Visualization: Ming Su, Shushi Peng
Writing - original draft: Shushi Peng, Zhaomin Dong
Writing – review & editing: Ming Su, Shushi Peng, Lili Chen, Bin Wang, Ying Wang, Zhaomin Dong

gross domestic product per capita (*GDPp*) may help ease COVID-19. Thus, we deduced that different meteorological conditions, proportion of elder people in demography, and socioeconomic indicators could be the potential factors driving the variation in transmission rate between different regions.

Based on the lessons from HCoV-HKU1 and HCoV-OC43 from U.S. census regions, a recent study suggested that more humid climates and summer will not substantially alter pandemic growth (Baker et al., 2020). Using weighted random effects regression, COVID-19 pandemic growth is strongly associated with public health interventions rather than temperature by 27 March 2020 (Jüni et al., 2020). Whether seasonal change to warmer temperature in summer can reduce the transmission of COVID-19 remains uncertain (Baker et al., 2020; Jüni et al., 2020; NAS, 2020). To derive sensitivity of transmission rate to temperature from worldwide data is another goal of this study.

Based upon global daily reported cases, the aims of this pilot research are (1) to investigate timeline of transmission rate of COVID-19 for each region; (2) to explore the potential factors driving the variation of transmission rate of COVID-19 across the globe; and (3) to estimate the temperature sensitivity of transmission rate of COVID-19. To accomplish these goals, we first built a logistic model to simulate the number of COVID-19-infected patients for 277 regions across the globe. Then, we investigated transmission rate (R_t) throughout the timeline of COVID-19 outbreak in the 277 regions across the globe and lag between the date of policy intervention and the decrease in transmission rate. To explore the associated factors for transmission rate across the 277 regions, we correlated the transmission rate at the point of inflection (R_I) with socioeconomic status, demographic factors, and meteorological conditions. Finally, the sensitivity of R_I to temperature was estimated by multiple models ensemble, and the change in transmission rate only due to warmer temperature in the coming summer was evaluated based on historical summer meteorological records.

2. Data and Methods

2.1. Data

Four types of data were acquired for the main analysis: (1) the daily confirmed cases were obtained from the GitHub project (https://github.com/CSSEGISandData/COVID-19/) during the period 1 December 2019 to 14 April 2020; (2) location, population, people aged over 65 ($P_{elderly}$), area, life expectation (*LE*), the number of hospital beds (N_{beds}), and *GDPp* for each region were requested from the World Bank open database (https://data.worldbank.org/); (3) the dates when strict control policies were implemented, typically border closure, strict travel restrictions/ban, and/or a state of emergency was declared were reviewed and summarized, given that the roles of the policy interventions were demonstrated in restricting the COVID-19 transmission (Chinazzi et al., 2020; Kucharski et al., 2020; Viner et al., 2020); and (4) the in situ observed humidity, temperature, wind speed, and visibility data were derived from the Global Historical Climatology Network (https://www.ncdc.noaa.gov/ghcn-daily-description). For China, United States, Australia, and Canada, the data were specified at province/state level, while data for other regions were assembled at country scale.

2.2. Statistical Analysis

A three-parameter logistic model was employed to describe the daily growth number:

$$y \sim a\ /(1 + \exp(b + c \times t)) \tag{1}$$

where y is the number of cases in millions; t is the time from 1 December 2019 in days; and a, b, and c are tubing parameters. Given that the virus spread in China has been in a stationary state since March, only daily data up to 1 March 2020 were utilized, with the exclusion of the infection wave in prisons. For the remaining countries, the data were updated to 14 April 2020. Note that some regions have the second wave outbreak of COVID-19 during peer review of this manuscript. We only studied the initial wave of COVID-19 across the globe here, and the second wave is beyond the scope of this study and is not considered in this study.

As illustrated in Figure 1, the growth of COVID-19 generally has three phases: the initial lag, exponential phase, and stationary phase. The point of departure (DP) for the study period was selected as the date of

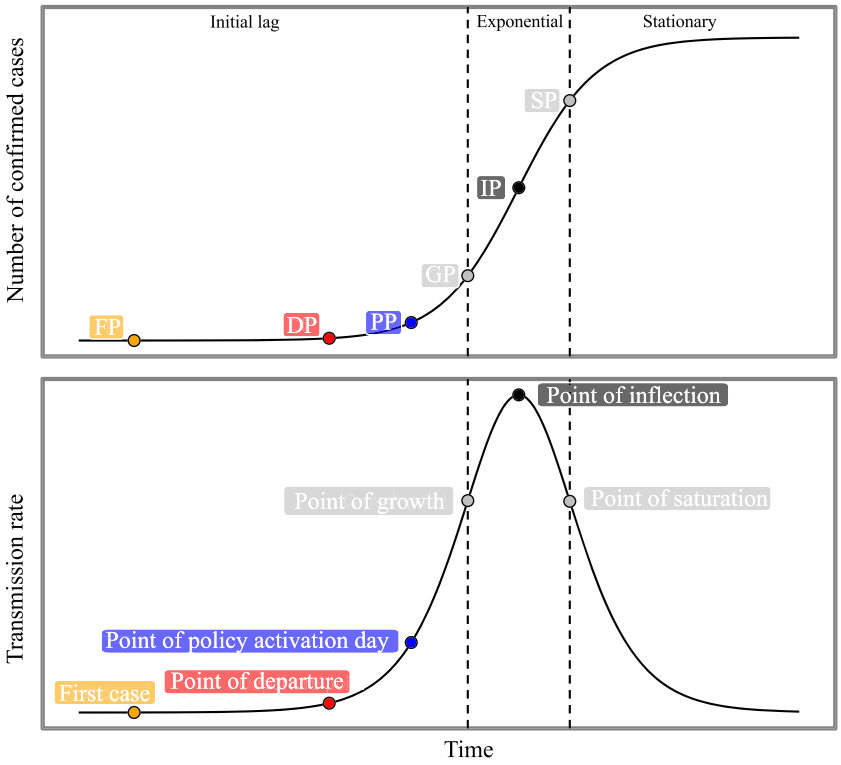

Figure 1. The schematic diagram of logistic model used in this study. IP (inflection point) is given by time of $max(R_t)$; GP (point of growth) and SP (point of saturation) are given by the time of $max(dR_t/dt)$ and $min(dR_t/dt)$, respectively. DP (point of departure) was assumed as five cases per million; PP, point of policy activation day. Detailed timeline for each region is provided in the supporting information.

five cases per million people (Figure 1). To validate the influence of this assumption, we also repeated our analysis by altering DP definition when case counts reached at 1 and 10 cases in per million, respectively.

In most regions, the model fitting is in good quantitative agreement with observations. The median of root mean square errors was calculated to be 9.7, with an interquartile range (IQR) of 36.4. We only chose regions with a visually sound fitness ($R^2 > 0.9$), and thus, the fitness for six regions were excluded. Finally, 50 states in the United States, 35 provinces/states/regions in China, 12 provinces in Canada, 8 states in Australia, and 172 other countries/regions were chosen as candidate regions for further analysis.

Then, the time-dependent transmission rate (R_t) was estimated based on the derivation of Equation 1:

$$Rt \sim -c \times a/(1+\exp(b+c\times t))^2 \times \exp(b+c\times t) \quad (2)$$

Here we chose the transmission rate at point of inflection (R_I) as a reliable indicator, as point of inflection (IP) is the middle of the exponential phase in the logistic growth curve (Figure 1), representing the maximum transmission rate. Then, we associated R_I with all collected demographic and socioeconomic variables, as well as meteorological factors.

2.3. Predictions of Transmission Rate Due To Temperature Change

In order to determine whether the summer will reduce the R_t or not naturally, we modeled the R_I based on an ensemble of multiple linear regressions (MLRs). We constructed an ensemble of multiple models with different combinations of independent variables, and for each model, we repeated the MLR 1,000 times with a randomly selected 70% of samples. Using this ensemble of multiple models, the change in R_t for July was predicted based on historical meteorological information.

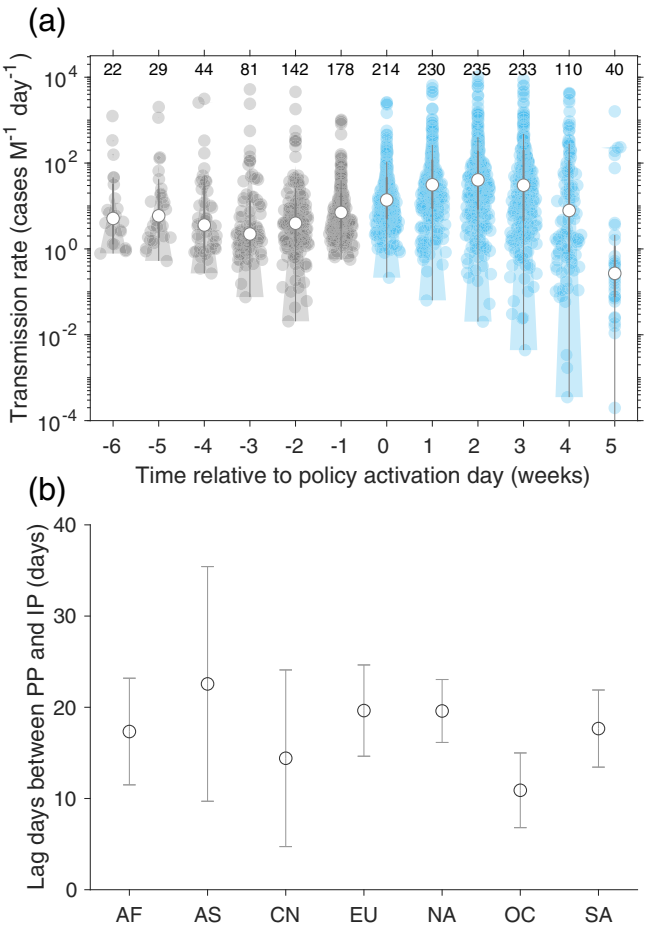

Figure 2. Transmission rate and lag between point of policy activation day (PP) and point of inflection (IP). (a) Changes in transmission rate with time relative to PP. (b) Lag days between PP and IP of transmission rate across the continents. The detailed definitions of PP and IP can be found in Figure 1. The regions are grouped into Africa (AF), Asia without China (AS), China (CN), Europe (EU), North America (NA), Oceania (OC), and South America (SA).

China has implemented strong policy interventions since January 2020 in more than 30 provinces. To avoid the effect from strong regulation on the R_t in China, data analyses were conducted under two scenarios: including and excluding Chinese data.

3. Results

3.1. The Timeline of COVID-19 Outbreak

The median calendar date for the first case report was 5 March 2020 (IQR: 21 days), and the R_t at the first reported case varied by 2 orders of magnitude across continents: 0.0327–0.571 cases M^{-1} day^{-1} (per million people per day). Later, the variation of R_t at GP was widened to a range of from 0.4 cases M^{-1} day^{-1} in Africa to 29.6 cases M^{-1} day^{-1} in Europe. Both duration and increased rate of Ln (R_t) between DP and GP accounted for the disparities of R_t at GP between continents (Figure S1). The longer duration between DP and GP resulted in larger R_t at GP in Europe than in Africa. The alternative definitions of DP (defined as the date when confirmed cases reached at 1 or 10 cases in per million) had similar results (Figures S2 and S3**)**. After GP, the R_t reached a peak after approximately 1 week as the median interval from GP to IP was 7 (IQR: 2) days globally, with small differences in the interval between continents (Figure S4**)**. The median calendar date for IP was 5 April 2020 (IQR: 9 days).

Further, we have collected the policy intervention details for 244 regions and examined the role of policy interventions in controlling the COVID-19 spread. Out of the 244 regions executing policy interventions, 161 did so within 2 weeks of the first reported case. Globally, the median duration between the first reported case and the point of policy activation date (PP) was 12 days (IQR: 20 days). In particular, the durations between the first reported case and PP for Asia without China, China, North America, South America, Africa, Europe, and Oceania were 23 (IQR: 42), 1 (IQR:1), 11 (IQR: 9), 13 (IQR: 12), 10 (IQR: 12), 19 (IQR: 37), and 20 (IQR: 35) days, respectively.

Figure 2a shows weekly R_t before and after policy interventions. At a global scale, the weekly R_t was fairly stable in the range 2.2–7.1 cases M^{-1} day^{-1} from 5 weeks to 1 week before PP. Then, the median R_t accelerated by 11.8 ± 3.1 (95% confidence interval [CI]: 5.8–17.8) cases M^{-1} day^{-1} per week until 2 weeks after PP (Figure 2a). After that, the median R_t dropped to 40.6 (IQR: 176.3) cases M^{-1} day^{-1} followed by 30.5 (IQR: 189.8) cases M^{-1} day in the third week. It then continuously decreased to 7.9 (IQR: 110.1) cases M^{-1} day^{-1} in the fourth week. In China (Figure S5), the weekly R_t started to drop about 1 week after PP, shorter than the global average.

In 241 out of 244 regions, IP was observed after the date of PP, indicating a lag resulting from the incubation period (i.e., the time delay from infection to illness onset) and/or the lag effect of policy interventions. A global median lag between PP and IP was determined to be 13.7 ± 15.2 (median: 18, IQR: 8) days. Figure 2b shows that the lag between PP and IP varied between continents: the value for Oceania was the lowest (median: 9 days with IQR of 4 days), compared to 13 (IQR: 3) days in China and 19 (IQR: 4) days in North America.

3.2. Global Distribution of R_I and the Associated Factors

The global median R_I (transmission rate at inflection point) was estimated of 9.4 (IQR: 33.3, n = 277) cases M^{-1} day^{-1}. Globally, the R_I varied by 4 orders of magnitude among countries, from 0.0094 to 585.6 cases M^{-1} day^{-1} (Figure 3). Across the 277 regions, the R_I in 14, 126, 110, and 27 regions were <0.1, 0.1–10, 10–100, and >100 cases M^{-1} day^{-1}, respectively. The R_I was the highest in Europe (median: 39.5, IQR: 88.7 cases M^{-1} day^{-1}, n = 46), followed by North America (median: 30.4, IQR: 44.6 cases M^{-1} day^{-1},

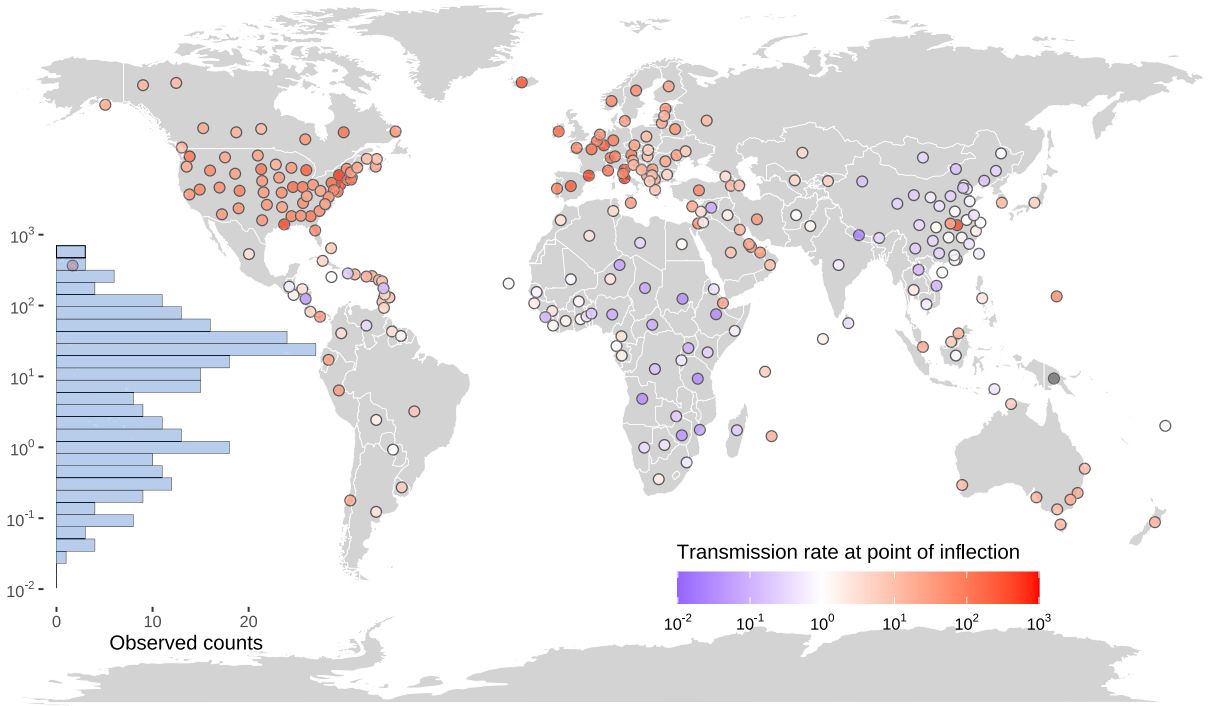

Figure 3. Spatial distribution of the transmission rate at point of inflection (R_I, cases M^{-1} day^{-1}). The inset bar plot shows the frequency of R_I in the 277 regions.

$n = 87$), Oceania (median: 11.5, IQR: 11.7 cases M^{-1} day^{-1}, $n = 12$), Asia without China (median: 3.8, IQR: 14.4 cases M^{-1} day^{-1}, $n = 38$), South America (median: 3.2, IQR: 9.6 cases M^{-1} day^{-1}, $n = 12$), China (median: 0.7, IQR: 0.8 cases M^{-1} day^{-1}, $n = 35$), and Africa (median: 0.5, IQR: 1.5 cases M^{-1} day^{-1}, $n = 47$).

We found that 1% increase in $P_{elderly}$ significantly enhanced R_I by 29.4% (25.2–34.0%) (Figure 4a), which supports that elderly people are more susceptible to SARS-CoV-2 (Verity et al., 2020). One-year uptick in *LE* is equal to 0.83 ± 0.046% growth in $P_{elderly}$ (Figure S6a), triggering 26.2% (95% CI: 22.4–30.1%) increment in R_I (Figure 4b). The regressions of R_I against *LE* and R_I against $P_{elderly}$ are similar when excluding data from China (Figure 4). The positive correlation between R_I and *GDPp* (Figure S7a) is due to the significant and positive correlations between *GDPp* and $P_{elderly}$ (Figure S6). No significant correlation is found for R_I with area per capita (Figure S7b).

Although relative humidity, wind speed, and visibility are positively associated with R_I (Figures 4c and S7), the explainable variances are all below 10%. For air temperature, Figure 4d shows a significant 7.7% (5.5–9.9%) decrease in R_I with per 1°C increase in air temperature across the 277 regions. When excluding Chinese regions, the temperature sensitivity of 7.7% (5.5–9.9%) increases to 10.9% (8.9–12.9%). This may be due to strong policy interventions in China lowering R_I and masking any temperature effect on R_I. We also did the same analysis with the R_t at GP and found similar results to those with the R_t at IP.

3.3. Temperature Sensitivity of R_I

We observed a significant correlation between temperature and $P_{elderly}$ (Figure S8). While this correlation is not a causal link, we speculated that the collinearities between temperature and $P_{elderly}$ would influence the temperature sensitivity of R_I. Thus, we first introduced the variable $P_{elderly}$ into the association of R_I with temperature, which led to a decrease in the regressed coefficient of temperature. Further, since the associations between LE, $P_{elderly}$, and *GDPp* factors and their high explainable variances for R_I (Figure 4), the combinations of *LE*, $P_{elderly}$, and *GDPp* variables were considered as confounding factors for determining the sensitivity of temperature to COVID-19 spread. The ensemble comprised a total of seven models (Table S1). However, the coefficients of air temperature were insignificant in all seven models when using global data. In Figure 4d, we speculated that the R_I in China could be largely suppressed by strong policy interventions in China rather than temperature across different provinces and may mask the possible

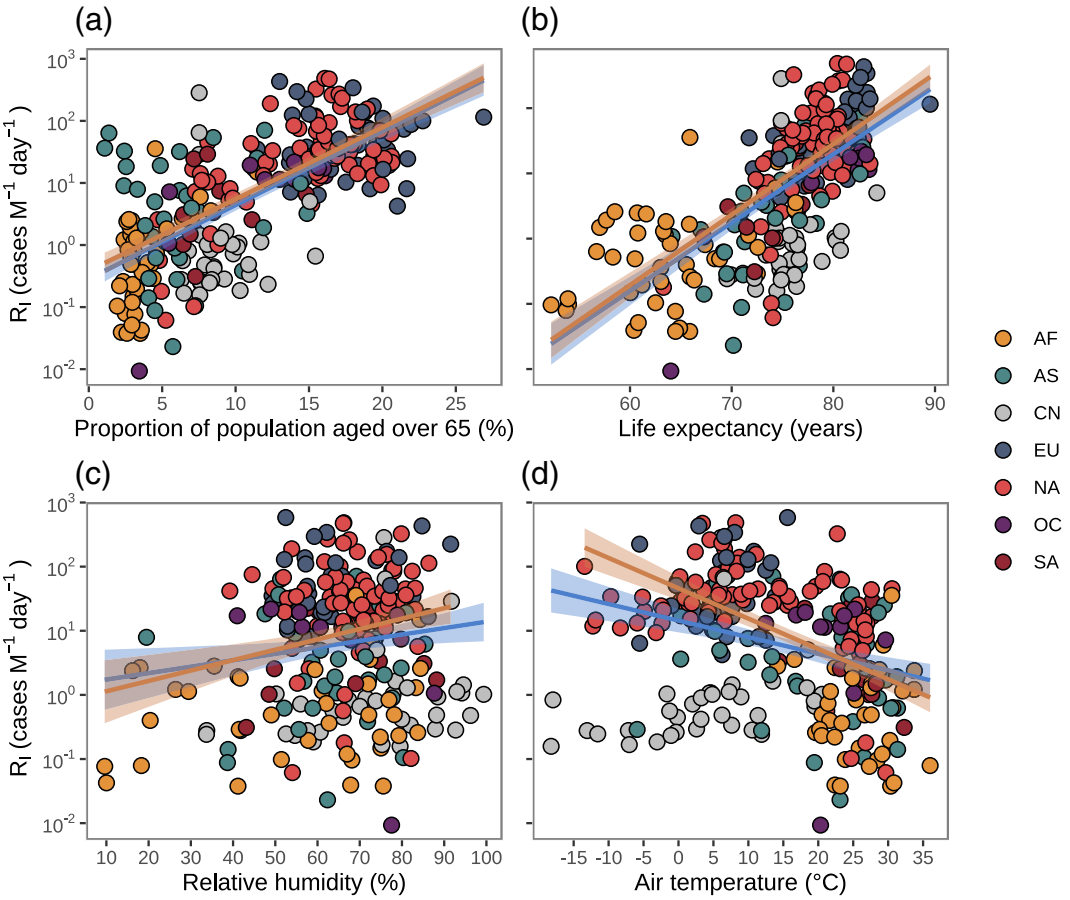

Figure 4. The association between transmission rate at point of inflection (R_I) and selected potential factors. (a) With proportion of population aged over 65 years: Ln (R_I) ~(25.83 ± 1.73) × x − (1.06 ± 0.22), $R^2 = 0.47$, $p < 0.0001$ for global data; Ln (R_I) ~(25.36 ± 1.65) × x − (0.82 ± 0.22), $R^2 = 0.51$, $p < 0.0001$ for global data without China. (b) With life expectancy: Ln (R_I) ~(0.23 ± 0.016) × x − (15.64 ± 1.17), $R^2 = 0.46$, $p < 0.0001$ for global data; Ln (R_I) ~(0.24 ± 0.014) × x − (16.00 ± 1.05), $R^2 = 0.57$, $p < 0.0001$ for global data without China. (c) With relative humidity: Ln (R_I) ~(0.021 ± 0.0090) × x + (0.39 ± 0.61), $R^2 = 0.020$, $p = 0.018$ for global data; Ln (R_I) ~(0.034 ± 0.0097) × x − (0.098 ± 0.64), $R^2 = 0.052$, $p = 0.0005$ for global data without China. (d) With air temperature: Ln (R_I) ~(−0.080 ± 0.012) × x + (3.01 ± 0.22), $R^2 = 0.14$, $p < 0.0001$ for global data; Ln (R_I) ~(−0.12 ± 0.012) × x + (3.91 ± 0.22), $R^2 = 0.51$, $p < 0.0001$ for global data without China. Blue and yellow lines with shade area show the fitness based on global data and global data without China, respectively. The colors of points indicate the regions in Africa (AF), Asia without China (AS), China (CN), Europe (EU), North America (NA), Oceania (OC), and South America (SA), respectively.

relationship between air temperature and R_I. We therefore examined the regressions excluding the data from China (Figure 4d). The coefficients of air temperature were then significant in four out of the seven models ($p < 0.05$), and we re-estimated temperature sensitivity between models ranging from −0.045 ± 0.010 to −0.010 ± 0.011 (unit: Ln [cases M^{-1} day^{-1}] per degree) (Table S2). Based on Monte Carlo sampling 1,000 times, a pooled estimation of coefficient was −0.027 ± 0.013 (95% CI: −0.052 to 4.81e-06, unit: Ln [cases per million per day] per degree, Figure S9), indicating that the R_I would decrease by 2.7% for per 1°C uptick in air temperature. Compared to the temperature sensitivity of R_I 10.9% (8.9–12.9%) obtained from the univariate regression between R_I and air temperature (Figure 4d), this substantial reduction can be explained by the high collinearities between temperature, $P_{elderly}$, LE, and $GDPp$ (Figure S8).

4. Discussion

We first summarized the timeline of the COVID-19 outbreak worldwide until 14 April 2020. The timeline of the COVID-19 outbreak in China provides a useful case to examine the effects of policy interventions. As

shown in Figure S1, the duration of the period between DP and GP was lower in China than in most other regions, but the increase of transmission rate during this period was relatively high, indicating a high early-stage risk in China. The combination of strictly enforced interventions at the community level, such as quarantine, travel ban/restriction, social distancing, home isolation, and others, sharply suppressed the basic reproduction number from 3.0 to less than 0.3 within 1 month (Pan et al., 2020). Integrated policy interventions led to lag days and R_I in China being 12.3 ± 3.2 days and 0.7 cases M^{-1} day^{-1}, respectively. These figures are lower than the median lag time and R_I in Asia or worldwide. If no or lesser policy interventions had been executed in China, the median R_I (based on *m7* in Table S1) was modeled to be 5.8 (IQR: 3.2) cases M^{-1} day^{-1}—8 times the actual median R_I in China (0.7 cases M^{-1} day^{-1}). From this, we can infer that the strong policy interventions in China reduced R_I by 88.5%. Lessons from Singapore also demonstrated how a mix of policies can substantially decrease the growth of COVID-19 infections (Koo et al., 2020). The policy of national school closure in 107 countries conducted by 18 March 2020 promised to prevent 2–4% of deaths (Viner et al., 2020). By model simulation, 90% travel restrictions only moderately affected the epidemic trajectory (Chinazzi et al., 2020; Viner et al., 2020) and warned that the implementation of a single or a couple of policies had less influence on the R_I. Modeling study in Italy also pointed out that restrictive social distancing should be implemented together with the widespread testing and contact tracing (Giordano et al., 2020). In Europe, it took longer from DP to GP and from GP to IP (Figures S1 and S4), as well as from PP to IP (Figure 2b). This could partly explain why R_I in Europe was the highest among the continents (Figure 3). Earlier PP and more strict policy interventions in Europe would have helped lower the R_I.

A study of 8,579 cases from 30 provinces in China stated that the proportion of cases in elderly people increased from 9% to 16% as epidemic evolved (Zhang et al., 2020), reinforcing the assertion that countries with a high proportion of older people need to take more action to quickly flatten the transmission curve in the early stage of the epidemic. In line with Zhang et al. (2020), our results show that 1% increase in $P_{elderly}$ increases R_I by 29.4% (25.2–34.0%) (Figure 4a). This suggests that people aged more than 65 years face ~2.5 times the infected risk faced by younger people in the context of the same infection probability. In addition, in Italy, the case fatality rate for people aged over 70 was in the range of 12.8–20.2%, which was much higher than the ratio of <3.5% for younger group (Onder et al., 2020). Retrospective clinical studies indicated that the proportion of lymphocytes for the elderly was markedly lower than that in the middle-aged group, indicating higher death risk for elderly patients with COVID-19 (Liu et al., 2020; Yang et al., 2020).

To examine the role of healthcare resources in controlling the COVID-19 pandemic, we evaluated how R_t changed as the epidemic proceeded. In the first 4 weeks, the R_t in countries with higher N_{beds} (>2.9 hospital beds per thousand) was 29.6 ± 15.1% higher than those countries with fewer N_{beds}. However, in the following weeks (Figure S10), the countries with higher N_{beds} lowered R_t, compared to continuous increasing R_t found in the countries with fewer N_{beds}. Overall, the increased rate of 0.099 ± 0.17 cases M^{-1} day^{-2} of Ln (R_t) in the countries with higher N_{beds} was lower than that of 0.79 ± 0.06 cases M^{-1} day^{-2} in the opposite group. A recent study pointed out that approximately 24% of countries have not adequately prepared for public health risks and events yet (Kandel et al., 2020). In Italy, the ratio of COVID-19 patients required intensive care was up to 16% (Grasselli et al., 2020), and the median days between symptom onset and critical care admission reached at 9 days in Wuhan, China by a single-centered, retrospective, observational study of 710 patients (Yang et al., 2020). In United States, scholars suggested that the COVID-19 outbreak was likely to cause the shortage of ICU beds, hospital beds, and ventilators (Emanuel et al., 2020). Thus, the rapid growth of COVID-19 in many regions could quickly overwhelm available resources, which calls for a global collaboration on building such health security capacity.

Previous studies suggested that environmental factors may affect the transmission rate of SARS-CoV and MERS-CoV (Baker et al., 2020; Chan et al., 2011; Van Doremalen et al., 2013), raising an expectation that high air temperatures could greatly reduce or even wipe out the COVID-19 pandemic. Mounting studies have also indicated that higher air temperature or humidity can markedly reduce the COVID-19 spread (e.g., Jüni et al., 2020; Qi et al., 2020). Study performed in Brazil indicated that air temperature only has a negative effect on confirmed cases below 25.8°C and has little effect above 25.8°C (Prata et al., 2020). In China, an early research stated that per temperature uptick would trigger 4.86% of increase in daily confirmed cases when temperature is below 3°C, while no decline effect was observed under warmer weather (Zhu & Xie, 2020). In contrast, another study conducted in China suggested a negative correlation between

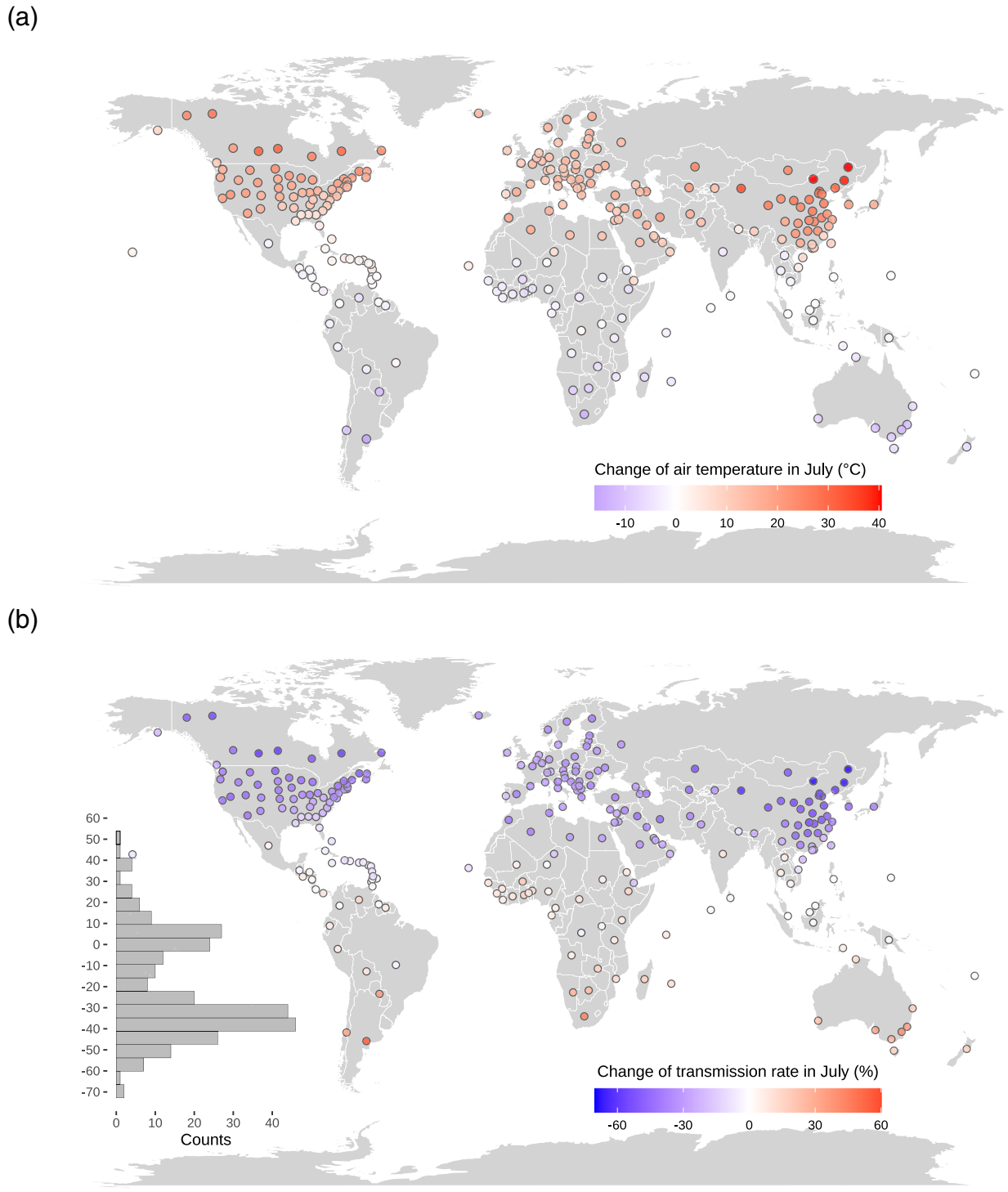

Figure 5. Change in summer temperature and change in transmission rate. (a) Change of air temperature between July 2019 and inflection point. (b) Relative differences of transmission rate due to change in temperature by the temperature sensitivity of transmission rate and the change in air temperature shown in Figure 5a. Note that this change in transmission rate only due to change in temperature is predicted, which is the product of temperature sensitivity of transmission rate and change in temperature.

air temperature and COVID-19 transmission rate (Qi et al., 2020). Previous studies did not examine whether collinearity between $P_{elderly}$ and air temperature causes the markedly negative temperature sensitivity of R_t. Here, after excluding the collinearities between $P_{elderly}$, LE, and $GDPp$ and temperature, the temperature sensitivity of R_I was substantially reduced by 75.6%. This suggests that previous estimates of the positive effect of air temperature on preventing transmission of COVID-19 may be exaggerated by univariate regression between COVID-19 transmission rate and temperature.

Imagining a world only shift to summer (July) temperature but keep other conditions unchanged (policy interventions, demography, etc.) as February and March, then the temperature sensitivity of R_I derived from the seven-model ensemble can be used to predict the relative change of R_I in this imagined world. An average 12.0 $\pm$ 8.9°C ($n = 239$) increase in air temperature in July was observed in the Northern Hemisphere, compared to a 5.2 $\pm$ 4.6°C ($n = 38$) decrease in the Southern Hemisphere (Figure 5a). Accordingly, due to temperature changes, the mean R_I was reduced by only 34.2 $\pm$ 25.9% in the Northern Hemisphere (Figure 5b), suggesting that the outbreak of COVID-19 would be marginally weakened in the coming summer. In contrast, the mean R_I was predicted to increase by 14.2 $\pm$ 12.5% in the Southern Hemisphere. This suggests that a warmer summer is unlikely to stop the transmission of COVID-19 naturally as the modeling study suggested (Baker et al., 2020) and that policy interventions, vaccine, and drugs for COVID-19 are crucial to cease the spread of COVID-19.

Some reports have implied that the number of confirmed cases is less than the number of real infections (Jia & Lu, 2020). A modeling study concluded that the weighted global ability to detect Wuhan-to-location imported infections of COVID-19 was only 38% of Singapore's capacity (Niehus et al., 2020). In many regions, only people with symptoms are prone or eligible for testing: unbiased testing should feature high testing counts and low positive rates. To explicate how testing counts impact our analysis, we defined a function as testing rate divided by positivity percentage to represent the data reliability of reported confirmed cases (Figure S11a). The median positivity rate in testing was 0.086 (IQR: 0.084) and tested counts were 8,337 (IQR: 11969) cases per million for 117 regions (Figure S11b). Statistical analysis based on data with high reliability **(**Figure S12 and Table S3**)** demonstrated that the LE, $P_{elderly}$, and $GDPp$ and temperature were still associated with R_I, and the coefficient was estimated to be -0.041 ± 0.016 ($p = 0.012$) for the association between Ln (R_I) and air temperature. In particular, based on data with high reliability, MLR shows 2.16% (95% CI: 0.23–4.00%) decrease in transmission rate per degree uptick in temperature, which is comparable to that based on all data. This confirms the robustness of the low temperature sensitivity of R_I estimated in this study and warns us that it would not be wise to expect the higher summer air temperatures to kill off the COVID-19 pandemic.

Several limitations of this study should be noted. First, our estimation of R_I was based on the reported number of confirmed cases. Although the re-analyses for countries with relatively high testing counts and low positive rate did not substantially alter our main findings, the variations of silent transmission between regions may bias our results. Second, an underlying assumption in our study is that the transmission rate before IP is marginally influenced by policy interventions because of the lag effect. Here, the duration between PP and IP was estimated to be 2 weeks. Considering the delays in reported cases, the latency of COVID-19, and test kit shortages in the early stage, our assumption may be fairly reasonable for countries with moderate or mild execution of policy interventions. However, for some countries like China, the strict implementation of policy interventions can sharply reduce R_I and mask the impacts of other factors. An accurate classification of the intensity of policy interventions could well enhance our study, although such classification is not available at this stage.

5. Conclusions

In this study, the timelines of COVID-19 outbreak show various lengths of the initial and exponential phases, among the global 277 regions. We summarized that the R_t reached a peak after approximately 1 week globally with little difference between the 277 regions. There were 161 out of 244 regions initiated policy interventions within 2 weeks of the first reported case. The maximum R_t at inflection point were found 2 weeks (IQR 8 days) after initiation of policy interventions and varied by 4 orders of magnitude among regions (0.0094 to 585.6 cases M^{-1} day^{-1}). This variation of R_I between the 277 regions is mainly explained by proportion of population aged over 65 or life expectancy (50%) and less by air temperature (~10%) across

the globe. The temperature sensitivity of R_I is derived from MRL as −2.7% (−5.2% to 0%) per degree Celsius, much smaller than that derived from univariate regression in which collinearity between air temperature and demographic factor is not considered. Due to the low temperature sensitivity of COVID-19 spread, our study suggests that the COVID-19 could be only marginally reduced naturally by warmer summer temperature. Before drugs and/or vaccine for COVID-19 come out, climatic seasonality has limited effect on transmission of COVID-19. Our study underscores the importance of policy interventions to cease the spread of COVID-19.

Conflict of Interest

The authors declare no conflicts of interest relevant to this study.

Data Availability Statement

The daily confirmed cases were obtained from the GitHub project (https://github.com/CSSEGISandData/COVID-19/) during the period 1 December 2019 to 14 April 2020; the demographic and socioeconomic variables, such as location, population, elderly people, life expectancy, area, GDP, and hospital beds were requested from the World Bank open database (https://data.worldbank.org/). The number of ICU beds per 10,000 was collected from Phua et al. (2020) and Rhodes et al. (2012). The in situ observed daily humidity, temperature, wind speed, and visibility data were derived from the Global Historical Climatology Network (https://www.ncdc.noaa.gov/ghcn-daily-description). The R language codes for main analyses can be publicly downloaded via archiving repository (https://zenodo.org/record/3964177 with a https://doi.org/10.5281/zenodo.3964177).

Acknowledgments
This study was supported by the National Natural Science Foundation of China (grant numbers 41722101, 42041003, and 51878649).

References

Baker, R. E., Yang, W., Vecchi, G. A., Metcalf, C. J. E., & Grenfell, B. T. (2020). Susceptible supply limits the role of climate in the early SARS-CoV-2 pandemic. *Science*, *369*(6501), 315–319. https://doi.org/10.1126/science.abc2535

Chan, K., Peiris, J., Lam, S., Poon, L., Yuen, K., & Seto, W. (2011). The effects of temperature and relative humidity on the viability of the SARS coronavirus. *Advances in Virology*, *2011*, 1–7. https://doi.org/10.1155/2011/734690

Chinazzi, M., Davis, J. T., Ajelli, M., Gioannini, C., Litvinova, M., Merler, S., et al. (2020). The effect of travel restrictions on the spread of the 2019 novel coronavirus (COVID-19) outbreak. *Science*, *368*(6489), 395–400.

Dehning, J., Zierenberg, J., Spitzner, F. P., Wibral, M., Neto, J. P., Wilczek, M., & Priesemann, V. (2020). Inferring change points in the spread of COVID-19 reveals the effectiveness of interventions. *Science*, *369*(6500), eabb9789. https://doi.org/10.1126/science.abb9789

Dong, E., Du, H., & Gardner, L. (2020). An interactive web-based dashboard to track COVID-19 in real time. *The Lancet Infectious Diseases*, *20*(5), 533–534. https://doi.org/10.1016/S1473-3099(20)30120-1

Emanuel, E. J., Persad, G., Upshur, R., Thome, B., Parker, M., Glickman, A., et al. (2020). Fair allocation of scarce medical resources in the time of COVID-19. *In: Mass Medical Soc.*, *2011*, 1–7. https://doi.org/10.1155/2011/734690

Giordano, G., Blanchini, F., Bruno, R., Colaneri, P., Di Filippo, A., Di Matteo, A., & Colaneri, M. (2020). Modelling the COVID-19 epidemic and implementation of population-wide interventions in Italy. *Nature Medicine*, 1–6.

Grasselli, G., Pesenti, A., & Cecconi, M. (2020). Critical care utilization for the COVID-19 outbreak in Lombardy, Italy: Early experience and forecast during an emergency response. *JAMA*, *323*(16), 1545–1546. https://doi.org/10.1001/jama.2020.4031

Jia, Z., & Lu, Z. (2020). Modelling COVID-19 transmission: From data to intervention. *The Lancet Infectious Diseases*, *20*(7), 757–758. https://doi.org/10.1016/S1473-3099(20)30258-9

Jüni, P., Rothenbühler, M., Bobos, P., Thorpe, K. E., da Costa, B. R., Fisman, D. N., et al. (2020). Impact of climate and public health interventions on the COVID-19 pandemic: A prospective cohort study. *CMAJ: Canadian Medical Association Journal*, *192*(21), 566–573.

Kandel, N., Chungong, S., Omaar, A., & Xing, J. (2020). Health security capacities in the context of COVID-19 outbreak: An analysis of international health regulations annual report data from 182 countries. *The Lancet*, *395*(10229), 1047–1053. https://doi.org/10.1016/S0140-6736(20)30553-5

Koo, J. R., Cook, A. R., Park, M., Sun, Y., Sun, H., Lim, J. T., et al. (2020). Interventions to mitigate early spread of SARS-CoV-2 in Singapore: A modelling study. *The Lancet Infectious Diseases*, *20*(6), 678–688. https://doi.org/10.1016/S1473-3099(20)30162-6

Kraemer, M. U., Yang, C.-H., Gutierrez, B., Wu, C.-H., Klein, B., Pigott, D. M., et al. (2020). The effect of human mobility and control measures on the COVID-19 epidemic in China. *Science*, *368*(6490), 493–497. https://doi.org/10.1126/science.abb4218

Kucharski, A. J., Russell, T. W., Diamond, C., Liu, Y., Edmunds, J., Funk, S., et al. (2020). Early dynamics of transmission and control of COVID-19: A mathematical modelling study. *The Lancet Infectious Diseases*, *20*(5), 553–558. https://doi.org/10.1016/S1473-3099(20)30144-4

Liu, K., Chen, Y., Lin, R., & Han, K. (2020). Clinical features of COVID-19 in elderly patients: A comparison with young and middle-aged patients. *Journal of Infection*, *80*(6), e14–e18. https://doi.org/10.1016/j.jinf.2020.03.005

NAS. (2020). Rapid expert consultation on SARS-CoV-2 survival in relation to temperature and humidity and potential for seasonality for the COVID-19 pandemic. NAS: National Academies of Sciences Engineering and Medicine., Available: https://www.nap.edu/catalog/25771/rapid-expert-consultation-on-sars-cov-2-survival-in-relation-to-temperature-and-humidity-and-potential-for-seasonality-for-the-covid-19-pandemic-april-7-2020. DOI: https://doi.org/10.1016/S2666-5247(20)30003-3.

Niehus, R., De Salazar, P. M., Taylor, A. R., & Lipsitch, M. (2020). Using observational data to quantify bias of traveller-derived COVID-19 prevalence estimates in Wuhan, China. *The Lancet Infectious Diseases*, *20*(7), 803–808. https://doi.org/10.1016/S1473-3099(20)30229-2

Onder, G., Rezza, G., & Brusaferro, S. (2020). Case-fatality rate and characteristics of patients dying in relation to COVID-19 in Italy. *JAMA*, *323*(18), 1775–1776. https://doi.org/10.1001/jama.2020.4683

Pan, A., Liu, L., Wang, C., Guo, H., Hao, X., Wang, Q., et al. (2020). Association of public health interventions with the epidemiology of the COVID-19 outbreak in Wuhan, China. *JAMA*, *323*(19), 1915–1923. https://doi.org/10.1001/jama.2020.6130

Phua, J., Faruq, M. O., Kulkarni, A. P., Redjeki, I. S., Detleuxay, K., Mendsaikhan, N., et al. (2020). Critical care bed capacity in Asian countries and regions. *Critical Care Medicine*, *48*(5), 654–662. https://doi.org/10.1097/CCM.0000000000004222

Prata, D. N., Rodrigues, W., & Bermejo, P. H. (2020). Temperature significantly changes COVID-19 transmission in (sub) tropical cities of Brazil. *Science of the Total Environment*, *729*, 138862. http://www.sciencedirect.com/science/article/pii/S0048969720323792, https://doi.org/10.1016/j.scitotenv.2020.138862

Qi, H., Xiao, S., Shi, R., Ward, M. P., Chen, Y., Tu, W., et al. (2020). COVID-19 transmission in mainland China is associated with temperature and humidity: A time-series analysis. *Science of the Total Environment, 728*(1), 138778. DOI: 138710.131016/j.scitotenv.132020.138778.

Rhodes, A., Ferdinande, P., Flaatten, H., Guidet, B., Metnitz, P., & Moreno, R. (2012). The variability of critical care bed numbers in Europe. *Intensive Care Medicine*, *38*(10), 1647–1653. https://doi.org/10.1007/s00134-012-2627-8

Tian, H., Liu, Y., Li, Y., Wu, C.-H., Chen, B., Kraemer, M. U., et al. (2020). An investigation of transmission control measures during the first 50 days of the COVID-19 epidemic in China. *Science*, *368*(6491), 638–642. https://doi.org/10.1126/science.abb6105

Van Doremalen, N., Bushmaker, T., & Munster, V. (2013). Stability of Middle East respiratory syndrome coronavirus (MERS-CoV) under different environmental conditions. *Eurosurveillance, 18*(38), 20590. DOI: 20510.22807/21560-27917.es22013.20518.20538.20590.

Verity, R., Okell, L. C., Dorigatti, I., Winskill, P., Whittaker, C., Imai, N., et al. (2020). Estimates of the severity of coronavirus disease 2019: A model-based analysis. *The Lancet Infectious Diseases*, *20*(6), 669–677.

Viner, R. M., Russell, S. J., Croker, H., Packer, J., Ward, J., Stansfield, C., et al. (2020). School closure and management practices during coronavirus outbreaks including COVID-19: A rapid systematic review. *The Lancet Child & Adolescent Health*, *4*(5), 397–404. https://doi.org/10.1016/S2352-4642(20)30095-X

Yang, X., Yu, Y., Xu, J., Shu, H., Xia, J. a., Liu, H., et al. (2020). Clinical course and outcomes of critically ill patients with SARS-CoV-2 pneumonia in Wuhan, China: A single-centered, retrospective, observational study. *The Lancet Respiratory Medicine*, *8*(5), 475–481. http://www.sciencedirect.com/science/article/pii/S2213260020300795, https://doi.org/10.1016/S2213-2600(20)30079-5

Zhang, J., Litvinova, M., Wang, W., Wang, Y., Deng, X., Chen, X., et al. (2020). Evolving epidemiology and transmission dynamics of coronavirus disease 2019 outside Hubei province, China: A descriptive and modelling study. *The Lancet Infectious Diseases*, *20*(7), 793–802. https://doi.org/10.1016/S1473-3099(20)30230-9

Zhu, Y., & Xie, J. (2020). Association between ambient temperature and COVID-19 infection in 122 cities from China. *Science of the Total Environment, 724*(1), 138201. DOI: 138210.131016/j.scitotenv.132020.138201.